Chemical Science

ROYAL SOCIETY OF CHEMISTRY

EDGE ARTICLE

View Article Online
View Journal | View Issue

Cite this: *Chem. Sci.*, 2023, **14**, 7026

All publication charges for this article have been paid for by the Royal Society of Chemistry

Oxygen transfer reactivity mediated by nickel perfluoroalkyl complexes using molecular oxygen as a terminal oxidant†

Shubham Deolka, [a] R. Govindarajan, [a] Eugene Khaskin, [a] Serhii Vasylevskyi, [a] Janet Bahri, [a] Robert R. Fayzullin, [b] Michael C. Roy[a] and Julia R. Khusnutdinova *[a]

Received 10th April 2023
Accepted 3rd June 2023

DOI: 10.1039/d3sc01861j

rsc.li/chemical-science

Nickel perfluoroethyl and perfluoropropyl complexes supported by naphthyridine-type ligands show drastically different aerobic reactivity from their trifluoromethyl analogs resulting in facile oxygen transfer to perfluoroalkyl groups or oxygenation of external organic substrates (phosphines, sulfides, alkenes and alcohols) using O_2 or air as a terminal oxidant. Such mild aerobic oxygenation occurs through the formation of spectroscopically detected transient high-valent Ni^{III} and structurally characterized mixed-valent Ni^{II}–Ni^{IV} intermediates and radical intermediates, resembling O_2 activation reported for some Pd dialkyl complexes. This reactivity is in contrast with the aerobic oxidation of naphthyridine-based $Ni(CF_3)_2$ complexes resulting in the formation of a stable Ni^{III} product, which is attributed to the effect of greater steric congestion imposed by longer perfluoroalkyl chains.

Introduction

Oxidation of organic substrates using molecular oxygen as a terminal oxidant is an important process in many biological processes[1] and in industrial aerobic oxidation catalysis where oxygen or air is considered as an inexpensive, "green" oxidant that produces no hazardous waste products.[2] Precious metal catalysts have been extensively used in enabling aerobic oxidation of hydrocarbon substrates or stoichiometric O_2 activation, typically based on Pt,[3] Pd,[4] Ru,[5] Rh,[6] Ir,[7] *etc.* At the same time, metalloenzymes capable of aerobic oxygenation typically contain more abundant first row transition metals, which led to the development of bioinspired model complexes capable of O_2 activation, most commonly based on Cu,[8] Fe,[9] Mn,[10] and Co.[11] Although Ni is known to be present at the active site of several O_2-reactive enzymes,[12] examples of synthetic "nickel oxygenase" reactivity in which Ni complexes assist in the transfer of O-atoms from O_2 to a substrate remain scarce.[13] While Ni complex examples in oxidation catalysis using strong oxidants, such as peroxides, NaOCl, PhIO, or *meta*-chloroperbenzoic acid, are well known,[2a,14] their utilization in aerobic oxidation is often prohibited by the stability of Ni^{II} towards aerobic oxidation. At the same time, several recent examples of the generation of highly reactive Ni superoxide or peroxo-species indicate that such species can participate in O-transfer reactivity.[15] Only a few examples of direct aerobic oxidation of Ni^{II} to produce high valent Ni species in +3 or +4 oxidation states are known, often enabled by the use of multidentate macrocyclic,[16] scorpionate,[17] and redox non-innocent ligands,[15d] with only one example featuring a simple organometallic tris(norbornyl)Ni complex that produced Ni^{IV} at low temperature under O_2.[18] More recently, we reported facile aerobic oxidation of a bis(trifluoromethyl)Ni^{II} complex supported by simple bidentate naphthyridine or methyl-substituted naphthyridine ligands to form stable bis(trifluoromethyl)Ni^{III} complexes capable of Ni^{III}–CF_3 bond homolysis and $C(sp^2)$–H bond radical trifluoromethylation (Scheme 1a).[19] Later we found that longer fluoroalkyl chains can be transferred to organic substrates as well using naphthyridine-free Ni catalyst.[20]

In this work, we report that naphthyridine-supported Ni^{II} complexes containing longer-chain pentafluoroethyl and heptafluoropropyl ligands show distinctly different reactivity with O_2, leading to the formation of perfluorocarboxylates as main products formed *via* the formal removal of both α-fluorine atoms and O-atom transfer from O_2 (Scheme 1b). In the presence of organic substrates, facile oxygen-atom transfer reactivity was induced, leading to aerobic oxidation of stilbenes to epoxides and benzaldehyde (*via* C=C bond cleavage), aerobic oxidation of alcohols, and oxygenation of phosphines and sulfides in a stoichiometric manner. These Ni^{II} complexes present a unique mode of O_2 activation by perfluoroalkyl

[a]*Coordination Chemistry and Catalysis Unit Okinawa Institute of Science and Technology Graduate University, 1919-1 Tancha, Onna-son, 904-0495, Okinawa, Japan. E-mail: juliak@oist.jp*

[b]*Arbuzov Institute of Organic and Physical Chemistry, FRC Kazan Scientific Center, Russian Academy of Sciences, 8 Arbuzov Street, Kazan, 420088, Russian Federation*

† Electronic supplementary information (ESI) available. CCDC 2241816–2241824 and 2204584. For ESI and crystallographic data in CIF or other electronic format see DOI: https://doi.org/10.1039/d3sc01861j

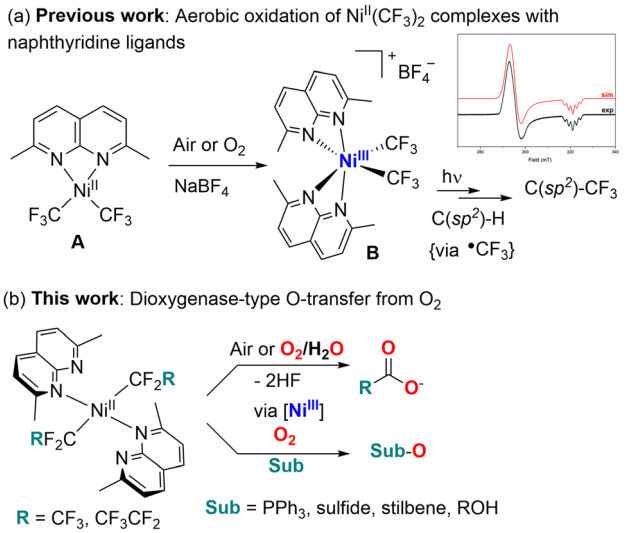

Scheme 1 Aerobic oxidation and reactivity of bis(trifluoromethyl) (a) and longer chain bis(perfluoroalkyl) complexes (b).

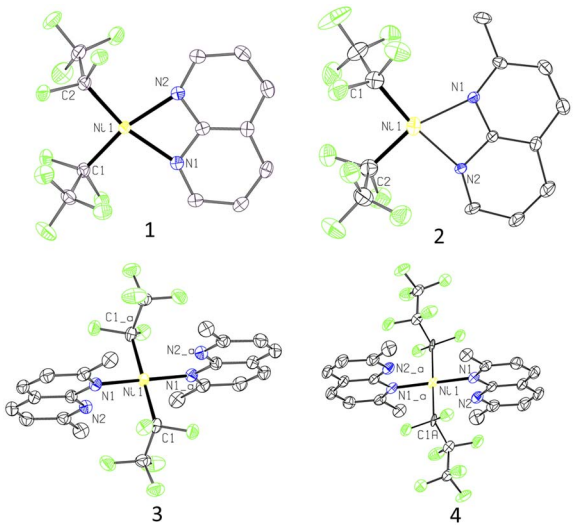

Fig. 1 ORTEP of 1, 2, 3, and 4 at the 60% probability level. The disorder for 2 and 4 as well as hydrogen atoms are omitted for clarity.

transition metal complexes that is unobserved in commonly studied trifluoromethyl analogs, and that leads to facile O-atom transfer reactivity and the formation of transient high valent Ni intermediates.

Results and discussion

Synthesis of longer chain Ni^{II} bis (perfluoroalkyl) complexes

First, complexation of 1,8-naphthyridine (**L1**) with (MeCN)$_2$-Ni^{II}(C$_2$F$_5$)$_2$ (ref. 21) precursor proceeds smoothly at room temperature (RT) in acetonitrile solution to give complex **1**, isolated in 58% yield and characterized by NMR, FT-IR, and UV/vis spectroscopy and electrospray ionization high-resolution mass spectrometry (ESI-HRMS) (Scheme 2). Single crystal X-ray diffraction (SC-XRD) study reveals that complex **1** contains one equivalent of **L1** coordinated to a Ni atom in a bidentate fashion with a Ni atom featuring a distorted square planar geometry, with geometry indices for four-coordinate structures $\tau_4 = 0.20$ and $\tau_4' = 0.19$ (the values for ideal square planar and ideal tetrahedral geometries are 0 and 1, respectively),[22] with *trans*-N–Ni–C bond angles of 166.08(9)° and 165.69(7)° (Fig. 1). Such distortion from square planarity is likely due to steric repulsion between *ortho*-H atoms of naphthyridine and fluorine atoms of the C$_2$F$_5$ group. Similarly, Vicic and co-workers reported that (4,4′-bis-*tert*-butyl-bipyridine)Ni(R^F)$_2$ (R^F = C$_2$F$_5$ or CF$_3$) complexes feature a distorted square planar geometry around Ni, which was attributed to interactions between fluorine atoms and *ortho*-H atoms of the ligand.[23] Among (4,4′-bis-*tert*-butyl-bipyridine)Ni(R^F)$_2$ series, a significantly greater degree of distortion was observed in a C$_2$F$_5$-analog compared to a trifluoromethyl complex implying that the introduction of a longer pentafluoroethyl chain imposes a notably greater steric hindrance compared to CF$_3$, while (bpy)NiMe$_2$ was essentially square planar.

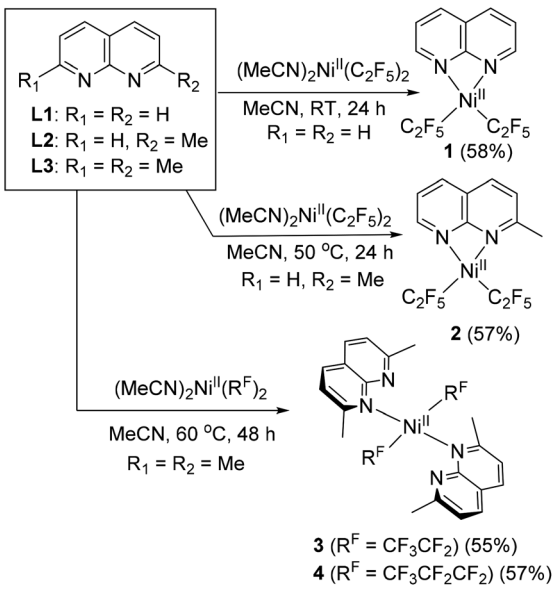

Scheme 2 Synthesis of Ni^{II} pentafluoroethyl and heptafluoropropyl complexes supported by naphthyridine ligand (isolated yields are shown in parentheses).

Interestingly, no complexation was observed at RT when more sterically hindered 2-methyl-1,8-naphthyridine (**L2**) was used, while further heating at 50 °C for 24 h afforded the yellow complex **2** with similar distorted square planar geometry and κ^2-coordinated **L2**.

Treatment of (MeCN)$_2$Ni^{II}(C$_2$F$_5$)$_2$ with the even more sterically hindered 2,7-dimethyl-1,8-naphthyridine **L3** at 60 °C resulted in the isolation of complex **3**. Surprisingly, SC-XRD reveals that two equivalents of κ^1-bound **L3** coordinate to the nearly ideally square planar ($\tau_4 = \tau_4' = 0.00$) Ni atom. The complex features two C$_2$F$_5$ groups in mutually *trans*-positions, with *trans*-N–Ni–N and C–Ni–C bond angles of 180°. This is strikingly different from the previously reported highly distorted square planar 1 : 1 complex (κ^2-**L3**)Ni^{II}(CF$_3$)$_2$ with

mutually *cis*-CF_3 groups ($\tau_4 = \tau_4' = 0.23$; C–Ni–N angle of 163.59(12)°). Such a configuration is uncommon for Ni^{II} dialkyl or bis(perfluoroalkyl) complexes due to the destabilizing presence of two strong *trans*-influencing ligands in *trans*-positions to each other (the *trans*-influencing properties of perfluoroalkyl group are expected to be similar to those of alkyl ligands).[23,24] In complex **3**, this unusual coordination mode is adopted to avoid steric congestion between two *ortho*-Me groups of **L3** and the bulkier C_2F_5 ligands, as supported by computational analysis (see Scheme S8 and Fig. S134 in the ESI†). Additional stabilization is achieved through the formation of an ideal square planar geometry preferred by a low spin Ni^{II} complex.

To examine if the same structural features will be observed in the complexes containing even longer perfluoroalkyl chains, we treated an analogous heptafluoropropyl $(MeCN)_2Ni^{II}(C_3F_7)_2$ (ref. 20) precursor with **L3** at 60 °C for 48 h, which led to the formation of complex **4**. SC-XRD reveals a similar, nearly ideal square planar structure with two *trans*-C_3F_7 groups and *trans*-N–Ni–N and C–Ni–C angles of 180°. Interestingly, both complexes **3** and **4** show well-resolved ^1H NMR spectra at RT in CD_2Cl_2 solution exhibiting only two **L3** ligand multiplets and one Me group, which could be due to the dynamic coordination of **L3**.

The Ni–C bonds in complex **3** (1.992(2) Å) are notably longer than in **1** (1.8904(19) and 1.899(2) Å), which is attributed to a stronger *trans*-influence between two C_2F_5 groups at 180°. Furthermore, Ni–C distances in longer-chain heptafluoropropyl complex **4** (2.021(6) Å) are slightly elongated compared to **3**.

Aerobic reactivity of complexes 2–4

We have previously reported that bis(trifluoromethyl) complexes $(\mathbf{L}')Ni^{II}(CF_3)_3$ ($\mathbf{L}'$ = **L1**, **L2**, and **L3**) undergo facile aerobic oxidation in the presence of air or O_2 and $NaBF_4$ at RT to produce isolable Ni^{III} complexes, $[(\mathbf{L}')Ni^{III}(CF_3)_2](BF_4)$ (Scheme 1a). In the case of longer-chain perfluoroalkyl analogs, we anticipated that different geometry around the Ni center and elongated Ni–C distances due to greater steric congestion could lead to a different reactivity in aerobic oxidation.

Since the attempted aerobic oxidation of complex **1** resulted in the release of a free ligand, we investigated the aerobic reactivity of complexes **2–4**. When solutions of **2–4** were exposed to O_2, no stable Ni^{III} product could be obtained, although the formation of a transient Ni^{III} species was detected spectroscopically at low temperature (*vide infra*). Surprisingly, when complexes **2–4** were exposed to air at RT for 2 h in *m*-xylene solution containing an additive of 5 equiv. of water, crystallization under ambient conditions afforded single crystals of trifluoroacetate complexes **2a–3a** and pentafluoropropionate complex **4a** isolated in 38–48% yields and analyzed by SC-XRD, ESI-HRMS, FT-IR, and UV/vis spectroscopy (Scheme 3 and Fig. 2). These complexes feature a pseudooctahedral geometry around a Ni coordinated to two (in **2a** and **4a**) or one (in **3a**) substituted naphthyridine ligand. Complexes **2a** and **3a** also contain coordinated water as terminal or bridging ligands, respectively. The Ni–O bond lengths in **2a** and **3a**, 2.0553(14) Å and 2.0758(10) Å, are consistent with typical Ni–O bond length in Ni^{II} aqua complexes,[25] while significantly shortened Ni distance (*ca.* 1.86–1.89 Å) is expected from Ni^{III}-hydroxo-bridged compounds.[26] The hydrogen atoms were placed onto coordinated water molecules and were freely refined, their position were determined from Fourier difference electron density maps (Fig. S130–S131).† The perfluorocarboxylate ligands in **2a–4a** retain the same number of carbon atoms, indicating that the carboxylate group is not formed *via* CO_2 insertion into the Ni–C bond but rather *via* a formal removal of two F-atoms from the Ni-bound difluoromethylene fragment.

The formation of perfluorocarboxylate products implies that free fluoride should be released into solution. This was

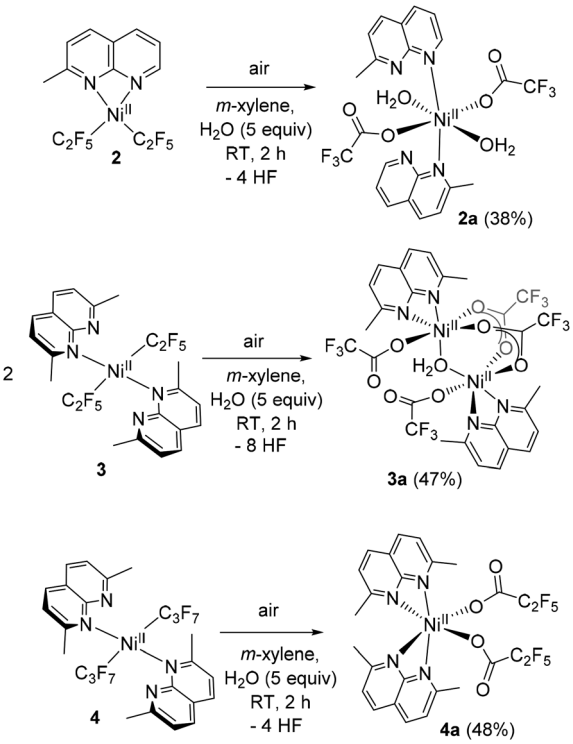

Scheme 3 Isolation of perfluorocarboxylate complexes by aerobic oxidation of **2-4** (isolated yields are shown in parentheses).

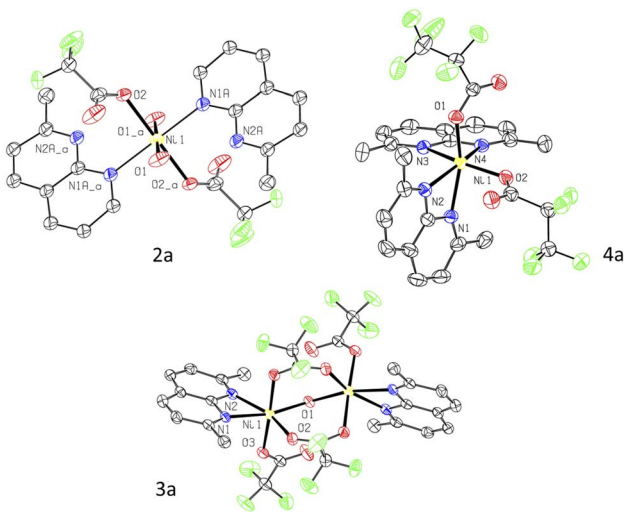

Fig. 2 ORTEP of **2a**, **3a**, and **4a** at the 60% probability level.

confirmed using a fluoride paper test (see ESI†). In addition, the formation of an unstable fluoride-bridged dinickel complex was confirmed by SC-XRD (*vide infra*).

To quantify the amount of perfluorocarboxylate formed during aerobic oxidation, we performed aerobic oxidation in a protic coordinating solvent, methanol, which could promote trifluoroacetate dissociation. The yield of diamagnetic fluorine-containing products was then determined by ^{19}F NMR integration against the internal standard, α,α,α-trifluorotoluene, and reported relative to the total number of available perfluoroalkyl groups (*i.e.*, two per Ni). Exposure of a MeOH-d_4 solution of **3** to ambient air at RT for 24 h produced a mixture of trifluoroacetate (70%) and pentafluoroethane (16%). Similarly, aerobic oxidation of **4** produced pentafluoropropionate (30%) and heptafluoropropane (38%). No oxidation was observed in MeOH solution of **3** under N_2, or in MeCN solution in the presence of 100 equiv. of water, and only starting material could be detected, showing that complex **3** is stable in protic solvents in the absence of oxygen. When the oxidation of **3** was performed under dry O_2 in methanol, the yield of trifluoroacetate increased to 76% (average for 2 trials), while no detectable amount of pentafluoroethane was observed.

To confirm the origin of O-atoms, we performed a series of experiments using ^{18}O-isotopically labeled reagents and analyzed the products by ESI-HRMS. First, two sets of peaks were detected in the control reaction mixture obtained by oxidation of **3** with unlabeled O_2 corresponding to cationic complexes of Ni with trifluoroacetate containing one or two **L3** ligands per Ni: $[(\mathbf{L3})Ni(CF_3COO)]^+$ (*m*/*z* 329.0037, calc. 329.0042) and $[(\mathbf{L3})_2Ni(CF_3COO)]^+$ (*m*/*z* 487.0880, calc. 487.0886) (Scheme 4a and Fig. S56†). The formation of both 2 : 1 and 1 : 1 complexes could be due to the labile nature of Ni^{II} complexes in solution and multiple modes of **L3** coordination. Next, when the oxidation of **3** was performed using $^{18}O_2$, the isotopic composition of these two peaks changes showing that the main product contained a doubly labeled trifluoroacetate, evident from the presence of the peaks corresponding to $[(\mathbf{L3})Ni(CF_3C^{18}O_2)]^+$ (*m*/*z* 333.0121, calc. 333.0127) and $[(\mathbf{L3})_2Ni(CF_3C^{18}O_2)]^+$ (*m*/*z* 491.0954, calc. 491.0971). The minor peaks were assigned to the analogous adduct with a singly labeled $CF_3C^{16}O^{18}O^-$ (*m*/*z* 331.0079 and 489.0909), and the non-labeled product was present in only small amounts. The ratio of the peaks corresponding to adducts with $CF_3C^{18}O_2^-$, $CF_3C^{18}O^{16}O^-$, and $CF_3C^{16}O_2^-$ was 100 : 36 : 16 after 24 hours (Scheme 4b and Fig. S58†). Similarly, when the oxidation of heptafluoropropyl complex **4** was performed under the same conditions, the major peaks were assigned to the doubly labeled adduct as a major product, while singly and unlabeled isotopomers were present in smaller amounts (the $C_2F_5C^{18}O_2^-$: $C_2F_5C^{18}O^{16}O^-$: $C_2F_5C^{16}O_2^-$ ratio of 100 : 40 : 20 after 24 h) (Scheme 4c and Fig. S62†).

The presence of a singly labeled product could result either from isotopomeric O_2 impurities or more likely from adventitious water present in a solvent. To confirm this idea, we performed oxidation of **3** with O_2 in the presence of 10 equiv. of $H_2{}^{18}O$, which resulted in the formation of a singly labeled $CF_3C^{18}O^{16}O^-$ adduct as a major product (Scheme 4d), while the analogous reaction under $^{18}O_2$ with 10 equiv. of unlabeled water produced singly labeled adduct and doubly labeled adduct in 100 : 8 ratio (Scheme 4e). These results suggest that when excess

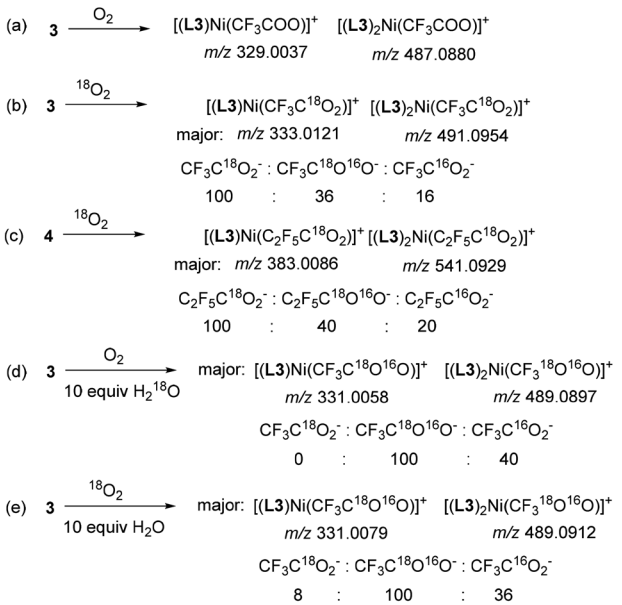

The ratio of CF_3COO isotopomers is shown as the ratio of peak intensities of a 2:1 adduct $[(\mathbf{L3})_2Ni(CF_3COO)]^+$; however, similar results were obtained if 1:1 adduct $[(\mathbf{L3})Ni(CF_3COO)]^+$ peaks were used.

Scheme 4 Reactivity of **3** and **4** with labeled O_2 and water.

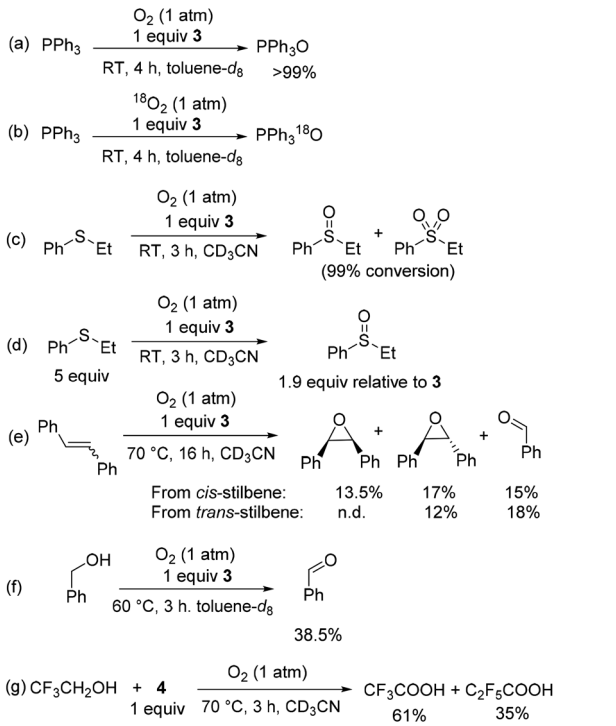

Scheme 5 Substrate oxidation in the presence of O_2 and complexes **3** or **4** under stoichiometric condition. Average yields are reported for 2–4 experiments.

water is introduced into a reaction mixture, it serves as a source of one of the O-atoms, while in the absence of added water, second oxygen atoms originate from O_2 or O_2-derived products (*e.g.*, peroxides or hydroxide).

Intrigued by this dioxygenase-type reactivity, we examined if oxygen transfer from O_2 could be directed to organic substrates in the presence of a suitable O-atom acceptor. Stirring solution of PPh_3 in the presence of 1 equiv. of **3** under an O_2 atmosphere at RT for 3–4 h afforded triphenylphosphine oxide with complete conversion (Scheme 5a). The PPh_3 oxidation in the presence of **3** and $^{18}O_2$ results in the formation of ^{18}O-labeled $Ph_3P^{18}O$ as a major product (90%) with only *ca.* 10% of unlabeled Ph_3PO present as confirmed by HRMS and GC-MS (Scheme 5b). One equivalent of **3** relative to PPh_3 was not required and using 0.5 equiv. **3** relative to PPh_3 resulted in *ca.* 95% conversion to PPh_3O after longer reaction time (20 h). Only a trace Ph_3PO product was observed during oxidation of PPh_3 with O_2 under analogous conditions in the absence of **3**.

Oxidation of phenyl ethyl sulfide in the presence of only 1 equiv. of **3** under O_2 atmosphere at RT produced a mixture of sulfoxide and sulfone at 99% conversion (Scheme 5c), whereas the analogous reaction with excess sulfide (5 equiv. relative to **3**) lead to a cleaner reaction that gave 1.9 equiv. of sulfoxide relative to **3** (Scheme 5d).

Heating a solution of *cis*-stilbene and 1 equiv. of **3** under O_2 at 70 °C for 16 h produced a mixture of *cis*-stilbene oxide (13.5%), *trans*-stilbene oxide (17%), and benzaldehyde (15%) along with unreacted starting material (Scheme 5e). Oxidation of *trans*-stilbene under O_2 in the presence of **3** produced *trans*-epoxide and benzaldehyde as main products in 12% and 18% average yields, respectively (Scheme 5e).

Oxidation of benzyl alcohol in the presence of 1 equiv. of **3** at 60 °C produced benzaldehyde in 38.5% yield after 3 h (Scheme 5f).

In the case of 2,2,2-trifluoroethanol oxidation, the unstable aldehyde intermediate was not detected and only the product of full oxidation, trifluoroacetic acid, was produced in 61% yield when 2,2,2-trifluoroethanol was heated under 1 atm of O_2 in the presence of complex **4** along with perfluoropropionate (35%) formed by C_3F_7 ligand oxidation (Scheme 5g).

During oxidation of PPh_3 or *trans*-stilbene in the presence of **3** and O_2, trifluoroacetate was detected only in minor amounts, 9–15%, showing that C_2F_5 groups might not be fully reacted when competitive oxygen acceptor was present. Although catalytic turnover has not yet been achieved, this might indicate the potential for substoichiometric use of nickel precursor in aerobic oxidation.

Overall, this reactivity shows that in the presence of suitable O-atom acceptors, activation of molecular oxygen by Ni perfluoroalkyl complexes resulted in oxidation or oxygenation of a number of substrates including phosphines, sulfides, alcohols, and alkenes.

Mechanistic investigation

To gain insight into the nature of possible high-valent Ni intermediates of O_2 activation with **3**, a solution of **3** in 2-methyltetrahydrofuran (2-MeTHF) was exposed to O_2 for 2 min and the resulting purple solution was frozen at 91 K and analyzed by EPR spectroscopy. An anisotropic signal was detected characterized by *g* values of 2.228, 2.206, and 2.023 showing splitting to a single N-atom ($A_N = 16.3$ G) (Fig. 3), which eventually disappears after warming up to RT at long reaction time. Significant *g* anisotropy and high *g* average values ($g_{ave} = 2.152$) are consistent with a Ni^{III} species similar to the previously reported complex **B** which shows splitting from two N-atoms (Scheme 1a; $A_N = 17.9$ G) (Scheme 1a, top right corner).[19] This implies that while complex **B** containing two *cis*-CF_3 groups is stabilized by two κ^2-**L3** ligands, similar κ^2-coordination of two **L3** ligands cannot be achieved upon oxidation of **3** and an exogenous ligand may be present. These differences could be attributed to a greater steric congestion around the Ni center in **3**. A similar signal was obtained upon exposure of complex **4** to O_2, showing superhyperfine splitting from only one N-atom (Fig. S105†).

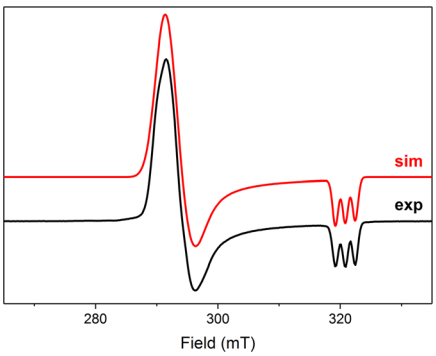

Fig. 3 Experimental X-band EPR spectra of the product of oxidation of **3** with O_2 (black line: MeTHF glass, 91 K, 9.082 GHz) and simulated EPR spectrum (red line). Simulation parameters: $g_x = 2.228$, $g_y = 2.206$, $g_z = 2.023$ ($A_N = 16.3$ G).

Such lack of stabilization by bis-ligation to two *cis* **L3** ligands could be imposed by steric congestion imposed by two *ortho*-Me groups of **L3** and bulky C_2F_5 ligands: for example, computational analysis shows that significant degree of steric congestion is present in a hypothetical *cis*-$(\mathbf{L3})_2Ni^{II}(C_2F_5)_2$ already in +2 oxidation state leading to significantly distorted structure and its destabilization compared to *trans*-configuration (see Scheme S8 and Fig. S134†).

When the aerobic oxidation of **3** was performed in the presence of 5,5-dimethyl-1-pyrroline *N*-oxide (DMPO) as a radical trap for O-derived radicals, no DMPO-OH adducts were observed suggesting that Fenton-type chemistry (*e.g. via* Ni-mediated $OH^{\bullet}$ radical formation by decomposition of O_2-derived H_2O_2) is unlikely to occur under these conditions, and the inner-sphere O_2 activation *via* superoxide formation may be involved in the initial oxidation to Ni^{III} (see Fig. S102†).[27]

Considering that *trans*-arrangement of two perfluoroalkyl groups will likely result in their greater reactivity in Ni–C bond homolysis, especially in Ni^{III} species, we then tested for the presence of the $C_2F_5^{\bullet}$ radical using the (2,2,6,6-tetramethylpiperidin-1-yl)oxyl (TEMPO) radical trap. When **3** was exposed to O_2 for 24 h at RT in the presence of TEMPO in CD_3OD, C_6D_6, or CD_3CN solutions, the TEMPO-C_2F_5 adduct

formed in 5–12% yields, while no TEMPO-C_2F_5 was detected in the absence of O_2, showing that aerobic oxidation is required for radical formation.[28]

Based on these observations, we propose that aerobic oxidation of **3** follows a radical pathway (Scheme 6), resembling the radical-chain mechanism for the oxidation of (bpy)$PdMe_2$ under O_2 pressure in the presence of AIBN radical initiator.[29] This mechanism is similar to the radical autooxidation of main group organometallics;[30] however, intermediates featuring Ni in higher oxidation states are accessible.

The initiation step involves the formation of an unstable Ni^{III} species, whose presence was confirmed by an EPR experiment (Fig. 3). Due to steric congestion and the mutual *trans*-configuration of two strong *trans*-influencing perfluoroalkyl groups in the starting material, such complexes are expected to be significantly less stable as compared to the previously reported *cis*-$[(\mathbf{L3})_2Ni^{III}(CF_3)_2]^+$ and likely to undergo facile, spontaneous Ni^{III}–C bond homolysis to produce a perfluoroalkyl radical **B** (Scheme 6a). In a propagation sequence, perfluoroalkyl radical **B** reacts with O_2, an efficient radical trap for alkyl radicals, to produce the perfluoroalkylperoxyl radical **C** (Scheme 6b).[31,32]

Haloalkyl peroxyl radicals have been reported to form in aerated solutions containing parent haloalkyl radicals, and they are known to act as efficient one-electron oxidants for metal complexes and organic substrates; such electron transfer may occur *via* an inner sphere mechanism and result in the formation of halogenated alkylperoxide anion.[31a,33] For example, oxidation of porphyrin metal complexes by $CF_3OO^{\bullet}$ radical resulting in one-electron oxidation of a metal center and trifluoroperoxide formation has been previously reported in the literature.[31a,34] By analogy, such reactivity between **C** and an easily oxidized Ni^{II} bis(perfluoroalkyl) complex would result in the formation of a Ni^{III} intermediate **D** (Scheme 6c) or, upon displacement of an electron-poor perfluoroalkylperoxo ligand with a protic solvent, intermediate **E** and free perfluoroalkyl hydroperoxide (Scheme 6d).[35] Further propagation involves the extrusion of perfluoroalkyl radical **B** from a Ni^{III} intermediate **D** or **E** (Scheme 6e) *via* a Ni–C bond homolysis.

Further decomposition of perfluoroalkyl hydroperoxide **F** is likely responsible for the carboxylate formation in the presence of a protic solvent or adventitious water from air *via* Path (i) or Path (ii) (Scheme 6). While there is currently no reported data on the hydrolytic stability of perfluoroalkyl hydroperoxides, 1,1-dichloroethyl peroxide is known to undergo spontaneous reaction with water to give peracetic acid and eventually acetic acid with the release of HCl.[36] Similar decomposition of perfluoroalkyl hydroperoxide **F** *via* Path (i) would then result in the formation of the corresponding carboxylic acid (Scheme 6f).

Alternatively, considering the ability of many transition metal complexes to catalyze alkylhydroperoxide disproportionation to alcohol and O_2, Path (ii) could involve Ni-catalyzed disproportionation of perfluorohydroperoxide to form a corresponding perfluorinated alcohol **G** (Scheme 6g).[37] The ability of **3** to catalyze hydroperoxide decomposition was confirmed in the experiment with cumene hydroperoxide (see ESI†) and was reported for other Ni^{II} complexes.[38] Both perfluoroethanol and perfluoro-*n*-propyl alcohol are known to be highly unstable and were characterized only in equilibrium mixtures with HF and the corresponding acyl fluoride (**H**) formed *via* thermodynamically favorable HF elimination.[39] The formation of easily hydrolyzed acyl fluoride **H** in the presence of protic solvents or adventitious water is expected to result in the formation of trifluoroacetic acid as a final product (Scheme 6h).[40] The formation of a singly-labeled trifluoroacetate as a major product in an experiment that involves $^{18}O_2/H_2O$ or $O_2/H_2{}^{18}O$ is also consistent with the proposed mechanism.[41]

Depending on the nature of the substrate, the O-transfer reactivity with organic substrates in the presence of **3** and O_2 could ultimately be due to the formation of perfluoroalkylperoxo species, which could be present either in high valent Ni-ligated form such as intermediate **D**[13a,15b,15d] (or oxo/hydroxo species resulting from subsequent O–O bond cleavage) or as free radicals upon their release into solution, both of which are known to be able to transfer oxygen atom to phosphines.[30]

Stilbene oxidation in the presence of O_2 and **3** (Scheme 5e) could also involve free radical reactivity or high valent Ni-ligated species: epoxide and aldehyde formation has been reported in free-radical alkene oxidation *via* alkylperoxy radical addition[42] or dioxetane intermediates, respectively.[43] However, considering that high valent Ni oxo or oxyl species have also been commonly proposed as intermediates in alkene epoxidation, these pathways cannot be clearly distinguished.[14a–g]

At the same time, the oxidation of alcohols likely involves the interaction of a Ni center directly with a substrate as no reaction was observed under free radical conditions in the absence of Ni.

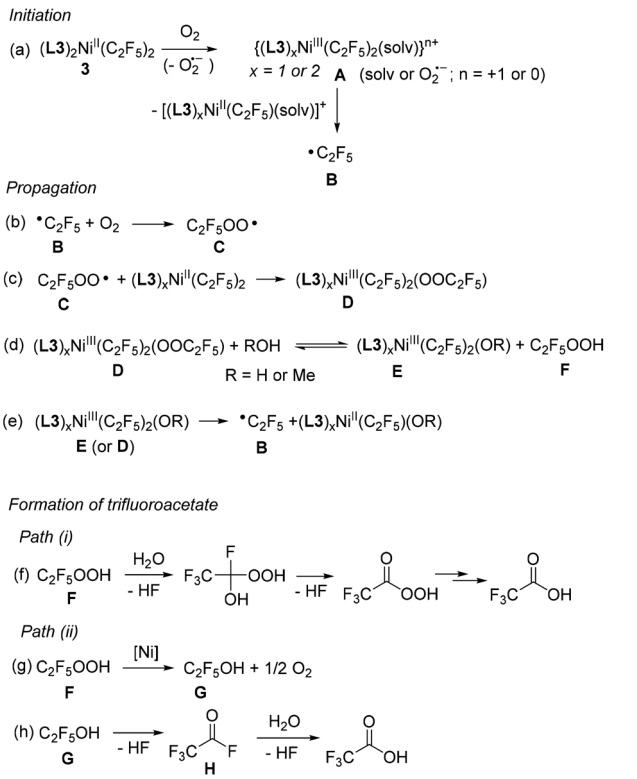

Scheme 6 Proposed mechanism for aerobic oxidation of **3**.

Detection of mixed-valent Ni^{IV}/Ni^{II} species

In an attempt to intercept high-valent intermediates, complex **3** was exposed to dry O_2 at −78 °C in CH_2Cl_2–MeCN solution. After 2 minutes, a purple paramagnetic solution formed, which showed an EPR signal (Fig. S106†) analogous to that in Fig. 3. Further slow crystallization from this solution for 2 weeks at −80 °C produced blue crystals of complex **5-MeCN** (Scheme 7 and Fig. 4). SC-XRD analysis of **5-MeCN** revealed the formation of a binuclear complex with two inequivalent Ni atoms bridged by three fluorine atoms; where one Ni atom is bound to three pentafluoroethyl groups, while another Ni atom coordinates to a κ^2-bound **L3** and one MeCN molecule. The analogous reaction in CH_2Cl_2-THF led to the crystallization of a similar THF-solvated **5-THF** (Fig. 4). The formation of bridging fluoride also confirms the presence of an extracted individual fluorine atom during aerobic oxidation of **3**.

Complexes **5-THF** and **5-MeCN** show distinctly different Ni1–F bonds around two Ni atoms,[44] with shorter Ni2–F bonds (1.910(4)–1.914(4) Å for **5-MeCN**, 1.9066(15)–1.9136(17) Å for **5-THF**) surrounding the $Ni(C_2F_5)_3$ center and longer Ni1–F bonds (1.968(6)–1.971(7) Å for **5-MeCN** and 1.998(17)–2.043(16) for **5-THF**) at the (**L3**)Ni(solv) center (Table 1). The Ni1–N bonds at the (**L3**)Ni(solv) center (2.097(2)–2.106(6) Å) are similar to those present in paramagnetic Ni^{II} complexes **2a–4a** (2.100(1)-2.182(2) Å) and are also similar to Ni^{II}–N bonds in high spin Ni^{II} complexes with N-donor ligands (2.045–2.095 Å),[45] while somewhat shorter Ni–N bonds may be expected from high-valent Ni complexes.[46] All three Ni2–C distances are similar (1.968(6) Å, 1.969(7) Å, and 1.971(7) Å in **5-MeCN**), suggesting pseudooctahedral coordination expected from Ni^{IV} rather than a Jahn–Teller distorted Ni^{III},[46,47] and similar to Ni^{IV}–CF_3 distances reported in the known Ni^{IV} complexes (1.960–2.016 Å).[46] Based on the highly inequivalent coordination properties

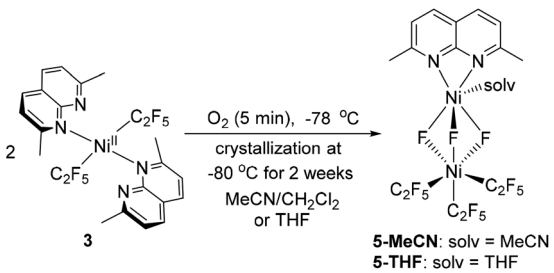

Scheme 7 Formation of **5-MeCN** and **5-THF**.

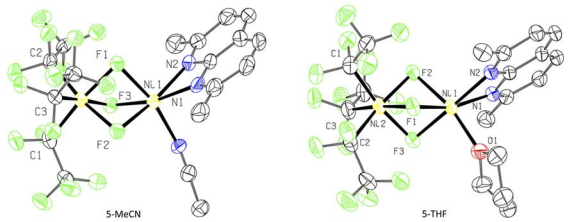

Fig. 4 ORTEP of **5-MeCN** (left) and **5-THF** (right) at the 50% probability level.[51]

Table 1 Selected interatomic distances in complexes **5-MeCN** and **5-THF** determined by SC-XRD[a]

Interatomic distance (Å)	5-MeCN	5-THF
Ni1–Ni2	2.6705(14)	2.6554(6)
Ni1–F1	2.045(4)	1.9982(17)
Ni1–F2	2.026(4)	2.0439(16)
Ni1–F3	2.006(4)	2.0118(16)
Ni1–N1	2.102(5)	2.097(2)
Ni1–N2	2.106(6)	2.108(2)
Ni1–O1	N. A.[b]	2.040(2)
Ni1–N3	2.020(5)	N. A.[b]
Ni2–F1	1.910(4)	1.9136(17)
Ni2–F2	1.913(4)	1.9066(15)
Ni2–F3	1.912(4)	1.9135(18)
Ni2–C1	1.972(7)	1.967(3)
Ni2–C2	1.968(6)	1.948(3)
Ni2–C3	1.969(7)	1.966(3)

[a] Atom numbering is according to Fig. 4. [b] N. A. – not applicable.

of each Ni center, complexes **5-MeCN** and **5-THF** can be assigned as Ni^{IV}/Ni^{II} mixed valent species, further supported by comparing the DFT-calculated relative stability of Ni^{IV}/Ni^{II} *vs.* the antiferromagnetically coupled Ni^{III}/Ni^{III} assignment for **5-MeCN**.

Complexes **5-THF** and **5-MeCN** likely result from a bimolecular alkyl group transfer in a follow-up reactivity after initial aerobic oxidation to Ni^{III}. Similarly, Me group transfer was reported during the oxidation of $PdMe_2$ complexes with N-donor ligands by ferrocenium or O_2, leading to the formation of $[(\mathbf{L}')Pd^{IV}Me_3]^+$ and $[(\mathbf{L}')Pd^{II}Me(solv)]^+$ ($\mathbf{L}'$ = 4,4′-bis-*tert*-butyl-2,2′-bipyridine or *N*,*N*′,*N*″-trimethyl-1,4,7-triazacyclononane).[48] Such alkyl group transfer has not been reported in the aerobic oxidation of Ni complexes; however, the formation of mixed trialkyl Ni^{IV} complexes by the direct radical attack at a Ni^{III} occurred when radicals were generated thermally using conventional free-radical initiators.[47b] Similarly, the alkyl radical attack at the metal center leading to its one-electron oxidation a new M-alkyl bond formation has been studied for other transition metal complexes.[35,49] Therefore, the formation of **5** represents a rare example of alkyl group transfer between Ni complexes induced by aerobic oxidation. Although complexes **5-solv** may not be directly involved in O-transfer reactivity, they demonstrate that mixed-valent complex formation may be viewed as a way to trap the C_2F_5 radical (as well as the HF byproduct) in the absence of a substrate. Interestingly, warming up the initially obtained purple solution obtained at low-temperature reaction of **3** with O_2 still results in the formation of **3a** as confirmed by SC-XRD, and trifluoroacetate formation is detected by NMR in the mixtures with protic solvents.[50]

Conclusions

Aerobic oxidation of perfluoroalkyl complexes containing perfluoroethyl or perfluoropropyl groups shows distinctly different reactivity from the analogous trifluoromethyl complexes, which

can be attributed to greater steric congestion imposed by longer-chain perfluoroalkyl groups. By contrast to trifluoromethyl complexes, stable Ni^{III} could not be obtained, although transient Ni^{III} intermediates were observed by EPR spectroscopy. In the absence of an external substrate, perfluorocarboxylate complexes were formed by the transfer of O-atoms from O_2 to the perfluoroalkyl group. Isotopic labeling studies suggest that in the absence of added water, O_2 serves as a major source of both O-atoms in the carboxylate product *via* dioxygenase-like reactivity, while in the presence of excess water, only one of the O-atoms originates from O_2.

Oxygenation of phosphine, sulfide, and stilbenes by O_2 as a terminal oxidant was also achieved that was promoted by longer-chain perfluoroalkyl Ni complexes. Aerobic oxidation of alcohols was also observed under stoichiometric conditions.

Overall, these results demonstrate that longer-chain perfluoroalkyl metal complexes may show drastically different reactivity from their commonly studied trifluoromethyl analogs. In the case of Ni complexes with naphthyridine ligands, such reactivity led to the observation of dioxygenase-like O-atom transfer from dioxygen under mild conditions.

Data availability

Data supporting this article have been uploaded as ESI.†

Author contributions

SD and JK designed the study, interpreted the data, and wrote the manuscript; RG and JB performed ligand synthesis; SV, EK and RF collected and refined crystallographic data; MR helped to carry out the mass spectrometry measurements; JK performed EPR experiments and computational analysis. All authors contributed in manuscript writing and editing.

Conflicts of interest

There are no conflicts to declare.

Acknowledgements

The authors thank the Instrumental Analysis section and Engineering section for technical support, the HPC facility for access to computational resources, and OIST for funding. R. R. F. performed crystal structure determination within the assignment for the Kazan Scientific Center of RAS. The authors thank Dr Ayumu Karimata for GPC analysis.

Notes and references

1 X. Huang and J. T. Groves, *Chem. Rev.*, 2018, **118**, 2491–2553.
2 (*a*) G. B. Shul'pin, *J. Chem. Res.*, 2002, **2002**, 351–353; (*b*) A. S. Hay, *J. Org. Chem.*, 1962, **27**, 3320–3321; (*c*) S. S. Stahl, *Angew. Chem., Int. Ed.*, 2004, **43**, 3400–3420; (*d*) L. Que and W. B. Tolman, *Nature*, 2008, **455**, 333–340.
3 (*a*) J. S. Valentine, *Chem. Rev.*, 1973, **73**, 235–245; (*b*) D. D. Wick and K. I. Goldberg, *J. Am. Chem. Soc.*, 1999, **121**, 11900–11901; (*c*) V. V. Rostovtsev, L. M. Henling, J. A. Labinger and J. E. Bercaw, *Inorg. Chem.*, 2002, **41**, 3608–3619; (*d*) J. R. Khusnutdinova, P. Y. Zavalij and A. N. Vedernikov, *Organometallics*, 2007, **26**, 2402–2413; (*e*) R. A. Taylor, D. J. Law, G. J. Sunley, A. J. P. White and G. J. P. Britovsek, *Angew. Chem., Int. Ed.*, 2009, **48**, 5900–5903; (*f*) A. R. Petersen, R. A. Taylor, I. Vicente-Hernández, P. R. Mallender, H. Olley, A. J. P. White and G. J. P. Britovsek, *J. Am. Chem. Soc.*, 2014, **136**, 14089–14099; (*g*) L. Xu, D. P. Solowey and D. A. Vicic, *Organometallics*, 2015, **34**, 3474–3479; (*h*) H. E. Zeitler, W. A. Kaminsky and K. I. Goldberg, *Organometallics*, 2018, **37**, 3644–3648.
4 (*a*) M. M. Konnick, I. A. Guzei and S. S. Stahl, *J. Am. Chem. Soc.*, 2004, **126**, 10212–10213; (*b*) J. M. Keith, R. P. Muller, R. A. Kemp, K. I. Goldberg, W. A. Goddard and J. Oxgaard, *Inorg. Chem.*, 2006, **45**, 9631–9633; (*c*) D. Wang, A. B. Weinstein, P. B. White and S. S. Stahl, *Chem. Rev.*, 2018, **118**, 2636–2679.
5 R. Neumann and M. Dahan, *Nature*, 1997, **388**, 353–355.
6 (*a*) C. M. Frech, L. J. W. Shimon and D. Milstein, *Helv. Chim. Acta*, 2006, **89**, 1730–1739; (*b*) J. M. Praetorius, D. P. Allen, R. Wang, J. D. Webb, F. Grein, P. Kennepohl and C. M. Crudden, *J. Am. Chem. Soc.*, 2008, **130**, 3724–3725; (*c*) E. C. Keske, O. V. Zenkina, A. Asadi, H. Sun, J. M. Praetorius, D. P. Allen, D. Covelli, B. O. Patrick, R. Wang, P. Kennepohl, B. R. James and C. M. Crudden, *Dalton Trans.*, 2013, **42**, 7414–7423.
7 (*a*) Z. M. Heiden and T. B. Rauchfuss, *J. Am. Chem. Soc.*, 2007, **129**, 14303–14310; (*b*) D. Bridget Williams, W. Kaminsky, J. M. Mayer and K. I. Goldberg, *Chem. Commun.*, 2008, 4195–4197; (*c*) S. Chowdhury, F. Himo, N. Russo and E. Sicilia, *J. Am. Chem. Soc.*, 2010, **132**, 4178–4190; (*d*) K. E. Allen, D. M. Heinekey, A. S. Goldman and K. I. Goldberg, *Organometallics*, 2014, **33**, 1337–1340; (*e*) M. Feller, E. Ben-Ari, Y. Diskin-Posner, R. Carmieli, L. Weiner and D. Milstein, *J. Am. Chem. Soc.*, 2015, **137**, 4634–4637; (*f*) P. Abril, M. P. del Río, J. A. López, A. Lledós, M. A. Ciriano and C. Tejel, *Chem.–Eur. J.*, 2019, **25**, 14546–14554.
8 (*a*) N. Kitajima and Y. Moro-oka, *Chem. Rev.*, 1994, **94**, 737–757; (*b*) E. I. Solomon, D. E. Heppner, E. M. Johnston, J. W. Ginsbach, J. Cirera, M. Qayyum, M. T. Kieber-Emmons, C. H. Kjaergaard, R. G. Hadt and L. Tian, *Chem. Rev.*, 2014, **114**, 3659–3853; (*c*) N. Gagnon and W. B. Tolman, *Acc. Chem. Res.*, 2015, **48**, 2126–2131; (*d*) C. E. Elwell, N. L. Gagnon, B. D. Neisen, D. Dhar, A. D. Spaeth, G. M. Yee and W. B. Tolman, *Chem. Rev.*, 2017, **117**, 2059–2107.
9 (*a*) M. Costas, M. P. Mehn, M. P. Jensen and L. Que, *Chem. Rev.*, 2004, **104**, 939–986; (*b*) T. L. Poulos, *Chem. Rev.*, 2014, **114**, 3919–3962; (*c*) S. Sahu and D. P. Goldberg, *J. Am. Chem. Soc.*, 2016, **138**, 11410–11428; (*d*) V. A. Larson, B. Battistella, K. Ray, N. Lehnert and W. Nam, *Nat. Rev. Chem.*, 2020, **4**, 404–419; (*e*) B. Battistella and K. Ray, *Coord. Chem. Rev.*, 2020, **408**, 213176.

10 (*a*) J. A. Kovacs, *Acc. Chem. Res.*, 2015, **48**, 2744–2753; (*b*) A. T. Fiedler and A. A. Fischer, *JBIC, J. Biol. Inorg. Chem.*, 2017, **22**, 407–424.

11 (*a*) D. Kim, J. Cho, Y.-M. Lee, R. Sarangi and W. Nam, *Chem.–Eur. J.*, 2013, **19**, 14112–14118; (*b*) T. Corona, S. K. Padamati, F. Acuña-Parés, C. Duboc, W. R. Browne and A. Company, *Chem. Commun.*, 2017, **53**, 11782–11785; (*c*) P. Liebing, F. Oehler, M. Wagner, P. F. Tripet and A. Togni, *Organometallics*, 2018, **37**, 570–583; (*d*) P. Kumar, S. V. Lindeman and A. T. Fiedler, *J. Am. Chem. Soc.*, 2019, **141**, 10984–10987.

12 (*a*) F. Al-Mjeni, T. Ju, T. C. Pochapsky and M. J. Maroney, *Biochem*, 2002, **41**, 6761–6769; (*b*) A. T. Fiedler, P. A. Bryngelson, M. J. Maroney and T. C. Brunold, *J. Am. Chem. Soc.*, 2005, **127**, 5449–5462; (*c*) J. L. Boer, S. B. Mulrooney and R. P. Hausinger, *Arch. Biochem. Biophys.*, 2014, **544**, 142–152; (*d*) Y.-J. Sun, Q.-Q. Huang and J.-J. Zhang, *Dalton Trans.*, 2014, **43**, 6480–6489; (*e*) J.-H. Jeoung, D. Nianios, S. Fetzner and H. Dobbek, *Angew. Chem., Int. Ed.*, 2016, **55**, 3281–3284.

13 (*a*) A. Company, S. Yao, K. Ray and M. Driess, *Chem.–Eur. J.*, 2010, **16**, 9669–9675; (*b*) A. T. Higgs, P. J. Zinn and M. S. Sanford, *Organometallics*, 2010, **29**, 5446–5449.

14 (*a*) J. D. Koola and J. K. Kochi, *Inorg. Chem.*, 1987, **26**, 908–916; (*b*) J. F. Kinneary, J. S. Albert and C. J. Burrows, *J. Am. Chem. Soc.*, 1988, **110**, 6124–6129; (*c*) J. F. Kinneary, T. R. Wagler and C. J. Burrows, *Tetrahedron Lett.*, 1988, **29**, 877–880; (*d*) H. Yoon and C. J. Burrows, *J. Am. Chem. Soc.*, 1988, **110**, 4087–4089; (*e*) H. Yoon, T. R. Wagler, K. J. O'Connor and C. J. Burrows, *J. Am. Chem. Soc.*, 1990, **112**, 4568–4570; (*f*) R. I. Kureshy, N. H. Khan, S. H. R. Abdi, P. Iyer and A. K. Bhatt, *J. Mol. Catal. A: Chem.*, 1998, **130**, 41–50; (*g*) R. I. Kureshy, N. H. Khan, S. H. R. Abdi, S. T. Patel, P. Iyer, E. Suresh and P. Dastidar, *J. Mol. Catal. A: Chem.*, 2000, **160**, 217–227; (*h*) T. Nagataki, Y. Tachi and S. Itoh, *Chem. Commun.*, 2006, 4016–4018; (*i*) Y. Morimoto, S. Bunno, N. Fujieda, H. Sugimoto and S. Itoh, *J. Am. Chem. Soc.*, 2015, **137**, 5867–5870; (*j*) Y. Qiu and J. F. Hartwig, *J. Am. Chem. Soc.*, 2020, **142**, 19239–19248.

15 (*a*) M. T. Kieber-Emmons, R. Schenker, G. P. A. Yap, T. C. Brunold and C. G. Riordan, *Angew. Chem., Int. Ed.*, 2004, **43**, 6716–6718; (*b*) M. T. Kieber-Emmons, J. Annaraj, M. S. Seo, K. M. Van Heuvelen, T. Tosha, T. Kitagawa, T. C. Brunold, W. Nam and C. G. Riordan, *J. Am. Chem. Soc.*, 2006, **128**, 14230–14231; (*c*) C. A. Rettenmeier, H. Wadepohl and L. H. Gade, *Chem. Sci.*, 2016, **7**, 3533–3542; (*d*) A. J. McNeece, K. A. Jesse, J. Xie, A. S. Filatov and J. S. Anderson, *J. Am. Chem. Soc.*, 2020, **142**, 10824–10832.

16 (*a*) F. Tang, N. P. Rath and L. M. Mirica, *Chem. Commun.*, 2015, **51**, 3113–3116; (*b*) S. M. Smith, O. Planas, L. Gómez, N. P. Rath, X. Ribas and L. M. Mirica, *Chem. Sci.*, 2019, **10**, 10366–10372.

17 N. Zhao, A. S. Filatov, J. Xie, E. A. Hill, A. Y. Rogachev and J. S. Anderson, *J. Am. Chem. Soc.*, 2020, **142**, 21634–21639.

18 V. Dimitrov and A. Linden, *Angew. Chem., Int. Ed.*, 2003, **42**, 2631–2633.

19 S. Deolka, R. Govindarajan, E. Khaskin, R. R. Fayzullin, M. C. Roy and J. R. Khusnutdinova, *Angew. Chem., Int. Ed.*, 2021, **60**, 24620–24629.

20 S. Deolka, R. Govindarajan, S. Vasylevskyi, M. C. Roy, J. R. Khusnutdinova and E. Khaskin, *Chem. Sci.*, 2022, **13**, 12971–12979.

21 C.-P. Zhang, H. Wang, A. Klein, C. Biewer, K. Stirnat, Y. Yamaguchi, L. Xu, V. Gomez-Benitez and D. A. Vicic, *J. Am. Chem. Soc.*, 2013, **135**, 8141–8144.

22 (*a*) L. Yang, D. R. Powell and R. P. Houser, *Dalton Trans.*, 2007, 955–964; (*b*) A. Okuniewski, D. Rosiak, J. Chojnacki and B. Becker, *Polyhedron*, 2015, **90**, 47–57; (*c*) D. Rosiak, A. Okuniewski and J. Chojnacki, *Polyhedron*, 2018, **146**, 35–41.

23 Y. Yamaguchi, H. Ichioka, A. Klein, W. W. Brennessel and D. A. Vicic, *Organometallics*, 2012, **31**, 1477–1483.

24 (*a*) V. V. Grushin and W. J. Marshall, *J. Am. Chem. Soc.*, 2006, **128**, 4632–4641; (*b*) R. E. Douthwaite, M. L. H. Green, P. J. Silcock and P. T. Gomes, *Organometallics*, 2001, **20**, 2611–2615; (*c*) I. Kieltsch, G. G. Dubinina, C. Hamacher, A. Kaiser, J. Torres-Nieto, J. M. Hutchison, A. Klein, Y. Budnikova and D. A. Vicic, *Organometallics*, 2010, **29**, 1451–1456.

25 (*a*) X. Meng, H. Hou, G. Li, B. Ye, T. Ge, Y. Fan, Y. Zhu and H. Sakiyama, *J. Organomet. Chem.*, 2004, **689**, 1218–1229; (*b*) G. Hu, N. Xiao, L. Wang, L. Shen, X. Li, H. Xu, L. Han and X. Xiao, *J. Solid State Chem.*, 2019, **270**, 247–251; (*c*) J. Z. Travis, C. J. LaRose and R. L. LaDuca, *Inorg. Chim. Acta*, 2017, **456**, 158–170.

26 A. Das, S. Chakraborty and S. K. Mandal, *Chem.–Asian J.*, 2021, **16**, 2257–2260.

27 (*a*) K. Reszka and C. F. Chignell, *Free Radical Res. Commun.*, 1991, **14**, 97–106; (*b*) G. R. Buettner, *Free Radical Biol. Med.*, 1987, **3**, 259–303; (*c*) I. Yamazaki and L. H. Piette, *J. Biol. Chem.*, 1990, **265**, 13589–13594.

28 The generation of free radicals during aerobic oxidation of **3** is also consistent with its ability to initiate polymerization of methylacrylate. Thus, reacting 1.5 μmol **3** and 1.5 μmol of O_2 with 1.5 mmol of methylacrylate for 16 h at 60 °C resulted in the formation of polymethylacrylate in 74% yield, while no polymerization was observed in the presence of O_2 without **3** or in the presence of **3** under N_2 with exclusion of O_2.

29 L. Boisvert, M. C. Denney, S. K. Hanson and K. I. Goldberg, *J. Am. Chem. Soc.*, 2009, **131**, 15802–15814.

30 A. G. Davies, *J. Chem. Res.*, 2008, **2008**, 361–375.

31 (*a*) P. Neta, R. E. Huie and A. B. Ross, *J. Phys. Chem. Ref. Data*, 1990, **19**, 413–513; (*b*) P. W. N. M. Van Leeuwen, H. Van Der Heijden, C. F. Roobeek and J. H. G. Frijns, *J. Organomet. Chem.*, 1981, **209**, 169–182; (*c*) J. K. Thomas, *J. Phys. Chem.*, 1967, **71**, 1919–1925; (*d*) L. C. T. Shoute, Z. B. Alfassi, P. Neta and R. E. Huie, *J. Phys. Chem.*, 1994, **98**, 5701–5704.

32 The bimolecular rate constant of an O_2 reaction with alkyl radicals is typically $\sim 109\ M^{-1}\ s^{-1}$. See ref. 31a.

33 (*a*) J. E. Packer, T. F. Slater and R. L. Willson, *Life Sci.*, 1978, **23**, 2617–2620; (*b*) J. E. Packer, R. L. Willson, D. Bahnemann and K.-D. Asmus, *J. Chem. Soc., Perkin Trans. 2*, 1980, 296–299; (*c*) D. Brault and P. Neta, *J. Phys. Chem.*, 1982, **86**,

3405–3410; (*d*) S. Mosseri, P. Neta and P. Hambright, *J. Phys. Chem.*, 1989, **93**, 2358–2362; (*e*) D. Brault and P. Neta, *J. Phys. Chem.*, 1984, **88**, 2857–2862; (*f*) D. Brault and P. Neta, *J. Phys. Chem.*, 1983, **87**, 3320–3327.

34 D. Brault and P. Neta, *J. Phys. Chem.*, 1987, **91**, 4156–4160.

35 A. Sauer, H. Cohen and D. Meyerstein, *Inorg. Chem.*, 1988, **27**, 4578–4581.

36 S. Gaeb and W. V. Turner, *J. Org. Chem.*, 1984, **49**, 2711–2714.

37 R. R. Hiatt, K. C. Irwin and C. W. Gould, *J. Org. Chem.*, 1968, **33**, 1430–1435.

38 (*a*) J. A. Howard and J. H. B. Chenier, *Can. J. Chem.*, 1976, **54**, 390–401; (*b*) H. Sigel, K. Wyss, P. Waldmeier and R. Griesser, *J. Coord. Chem.*, 1974, **3**, 235–247.

39 A. F. Baxter, J. Schaab, J. Hegge, T. Saal, M. Vasiliu, D. A. Dixon, R. Haiges and K. O. Christe, *Chem.–Eur. J.*, 2018, **24**, 16737–16742.

40 C. J. Young and S. A. Mabury, in *Reviews of Environmental Contamination and Toxicology Volume 208: Perfluorinated alkylated substances*, ed. P. De Voogt, Springer New York, New York, NY, 2010, pp. 1–109.

41 The possible mechanism of the formation of doubly labeled trifluoroacetate is discussed in detail in the ESI.†

42 Y. Wu, X. Tang, J. Zhao, C. Ma, L. Yun, Z. Yu, B. Song and Q. Meng, *ACS Sustainable Chem. Eng.*, 2020, **8**, 1178–1184.

43 (*a*) G.-Z. Wang, X.-L. Li, J.-J. Dai and H.-J. Xu, *J. Org. Chem.*, 2014, **79**, 7220–7225; (*b*) A. Rajagopalan, M. Lara and W. Kroutil, *Adv. Synth. Catal.*, 2013, **355**, 3321–3335.

44 To examine the possiblity of alternative assignments for fluorine atoms (e. g. hydroxide), when the type of bridging atoms was changed from fluorine to oxygen, the R-factors increased significantly. In this case, the volume of the thermal ellipsoids unnaturally decreased and positive residual peaks appeared very close to the nucleus. This usually indicates that an element with more electrons should be assigned (in this case, fluorine provided the best results). Moreover, when replacing fluorine with oxygen, no peaks of residual density are observed that could be attributed to the accompanying hydrogen atoms, although the quality of the data and their resolution are sufficient to expect them to appear.

45 (*a*) M. Garai, D. Dey, H. R. Yadav, A. R. Choudhury, N. Kole and B. Biswas, *Polyhedron*, 2017, **129**, 114–122; (*b*) I. Ucar, O. Z. Yesilel, A. Bulut, H. Olmez and O. Buyukgungor, *Acta Crystallogr., Sect. E: Struct. Rep. Online*, 2005, **61**, m947–m949.

46 F. D'Accriscio, P. Borja, N. Saffon-Merceron, M. Fustier-Boutignon, N. Mézailles and N. Nebra, *Angew. Chem., Int. Ed.*, 2017, **56**, 12898–12902.

47 (*a*) E. A. Meucci, S. N. Nguyen, N. M. Camasso, E. Chong, A. Ariafard, A. J. Canty and M. S. Sanford, *J. Am. Chem. Soc.*, 2019, **141**, 12872–12879; (*b*) J. R. Bour, D. M. Ferguson, E. J. McClain, J. W. Kampf and M. S. Sanford, *J. Am. Chem. Soc.*, 2019, **141**, 8914–8920.

48 (*a*) M. P. Lanci, M. S. Remy, W. Kaminsky, J. M. Mayer and M. S. Sanford, *J. Am. Chem. Soc.*, 2009, **131**, 15618–15620; (*b*) J. R. Khusnutdinova, F. Qu, Y. Zhang, N. P. Rath and L. M. Mirica, *Organometallics*, 2012, **31**, 4627–4630.

49 (*a*) J. H. Espenson, *Acc. Chem. Res.*, 1992, **25**, 222–227; (*b*) J. K. Kochi, *Acc. Chem. Res.*, 1974, **7**, 351–360; (*c*) N. Shaham, A. Masarwa, Y. Matana, H. Cohen and D. Meyerstein, *Eur. J. Inorg. Chem.*, 2002, **2002**, 87–92.

50 Allowing the purple reaction mixture obtained by low temperature oxidation of **3** with O_2 to warm up to RT only for 3–5 minutes led to the formation of yellow solution, from which a mixed F-bridged/TFA-bridged complex **6** (see ESI†), $[Ni(C_2F_5)_3(\mu\text{-}F)(\mu\text{-}OOCCF_3)2Ni(\kappa^2\text{-}\mathbf{L3})(THF)]$ was obtained by crystallization at −80 °C for 3 days. This complex is likely formed *via* F-displacement by trifluoroacetate accumulated in solution during room temperature reaction.

51 Deposition Numbers 2241816–2241824 and 2204584 contain the supplementary crystallographic data for this paper.